41 The Value of Positron Emission Tomography for Differentiating Brain Tumor Progression and Treatment-Induced Changes

Bart R. J. van Dijken, Roelien H. Enting, Hanne-Rinck Jeltema, Miranda C. A. Kramer, Rudi A. J. O. Dierckx, and Anouk van der Hoorn

Contents

B. R. J. van Dijken (✉) · A. van der Hoorn
Department of Radiology, Medical Imaging Center (MIC), University Medical Center Groningen, University of Groningen, RB, Groningen, The Netherlands
e-mail: b.r.j.van.dijken@umcg.nl

R. H. Enting
Department of Neurology, University Medical Center Groningen, University of Groningen, RB, Groningen, The Netherlands

H.-R. Jeltema
Department of Neurosurgery, University Medical Center Groningen, University of Groningen, RB, Groningen, The Netherlands

M. C. A. Kramer
Department of Radiotherapy, University Medical Center Groningen, University of Groningen, RB, Groningen, The Netherlands

R. A. J. O. Dierckx
Department of Nuclear Medicine and Molecular Imaging, Medical Imaging Center (MIC), University Medical Center Groningen, University of Groningen, RB, Groningen, The Netherlands

R. A. J. O. Dierckx et al. (eds.), *PET and SPECT in Neurology*,
https://doi.org/10.1007/978-3-030-53168-3_41

Abstract

Accurate differentiation of tumor progression and treatment-induced changes is the key to treatment decision in brain tumors. Several new tracer options are promising, of which [^{11}C]-methyl-L-methionine (MET) and O-(2-[^{18}F]-fluoroethyl)-L-tyrosine (FET) positron emission tomography (PET) are the most used. This chapter provides a clinical overview of important issues of treatment evaluation in primary brain tumors and brain metastases. The role and dilemmas in neuroimaging, including magnetic resonance imaging (MRI) and PET, are discussed. An overview is given of the role of MRI and PET in brain tumor follow-up with special focus on available literature in the role of amino acid PET to differentiate between tumor progression and treatment-induced changes.

41.1 Introduction

Malignant brain tumors are relatively uncommon tumors in adults, making up less than 2% of all cancer cases (DeAngelis 2001; Miranda-Filho et al. 2017). The two major groups are a heterogeneous group of primary brain tumors and cerebral metastases from systemic cancer, with the latter being more common (DeAngelis 2001). Brain tumors are responsible for a significant loss of healthy life years and impaired quality of life. Treatment is often aggressive trying to improve this outcome. During and after treatment, patients are monitored with imaging to assess treatment response and to decide whether the current treatment should be continued or not.

41.1.1 Primary Brain Tumors

Primary intra-axial brain tumors are most commonly gliomas (in approximately 80% of the cases), with the majority being grade IV glioblastoma (Ostrom et al. 2019). Less frequent intra-axial primary brain tumors are lymphomas (6% of cases) and embryonal tumors (in about 3%) (Ostrom et al. 2019; Louis et al. 2016). In this chapter, we focus on gliomas.

To determine the tumor grade of gliomas, historically, the WHO grading system is used, representing a malignancy scale varying from I to IV. Grade I lesions are regarded as benign tumors due to their low proliferative potential and curative intent of surgical resection alone. Grade II tumors represent low-grade tumors, and grade III and IV tumors are high-grade tumors, often associated with rapid disease evolution and a dismal survival.

Recently, the WHO grading system for brain tumors has been revised. Genetic and molecular markers have now become integral to the grading (Louis et al. 2016). Survival has been shown to be greatly dependent upon these molecular markers (Rogers et al. 2018; Bell et al. 2018; Binabaj et al. 2018). Diffuse gliomas, being astrocytomas and oligodendrogliomas, are defined based on their molecular profile. Currently, the most important molecular markers are mutations in the isocitrate dehydrogenase (IDH) genes, most often IDH-1 and sometimes IDH-2. They are associated with a better prognosis in lower-grade gliomas or secondary glioblastomas (Rogers et al. 2018). Low-grade gliomas are diffusely infiltrating and slow-growing. Low-grade astrocytomas are currently defined as IDH-1- or IDH-2-mutated tumors without a 1p/19q co-deletion (Louis et al. 2016). Oligodendrogliomas are both IDH-mutant and 1p/19q-co-deleted (Louis et al. 2016).

High-grade gliomas usually lack the aforementioned IDH mutations. Another important prognostic marker for high-grade gliomas is O6-methylguanine methyltransferase (MGMT) gene methylation status. Patients with an MGMT-methylated tumor are more susceptible to alkalizing chemotherapy such as temozolomide and thus have a better survival (Bell et al. 2018; Binabaj et al. 2018).

Patients with IDH-mutant grade II tumors or co-deleted gliomas have a median survival of 10+ years, and patients with a non-co-deleted WHO grade III tumor have a median survival of 5 years (van den Bent et al. 2017), in contrast with patients with IDH wild-type grade IV tumors with a median survival of 1 year. Unfortunately, high-grade gliomas account for over 70% of newly diagnosed gliomas (Ostrom et al. 2019).

Peak incidence of low-grade gliomas occurs in patients aged between 35 and 45 years (Weller et al. 2017). It is assumed that all low-grade gliomas will transform into high-grade gliomas. Current clinical practice of low-grade gliomas recommends early surgical resection when safely possible. This is followed by both radiotherapy and chemotherapy or a wait-and-scan policy. The latter is usually chosen in completely resected young patients (Weller et al. 2017).

Patients with glioblastoma have a median age of onset of approximately 60 years. Prognosis of patients with high-grade gliomas has remained poor for the last decades. Glioblastomas, as all gliomas, are infiltrating in nature, often involving eloquent structures, and extend beyond visual borders on imaging, making complete resection without unacceptable damage impossible (Boonzaier et al. 2017; Yan et al. 2019). Nevertheless, surgery remains the cornerstone in glioblastoma treatment. Patients with high-grade gliomas benefit from a greater extent of resection in terms of survival (Sanai and Berger 2008; Yan et al. 2017). The standard adjuvant treatment in patients in good general and neurological condition, aged up to 70 years, is 60 Gy radiotherapy with concomitant temozolomide chemotherapy followed by a six-course regimen of maintenance temozolomide chemotherapy (Stupp et al. 2005). Recurrence, however, is inevitable due to the inability of radical resection and subsequent resistance to chemoradiation therapy. Currently the median survival after standard treatment of chemoradiation is 14.9 months, with the biggest gain for patients with a methylated MGMT tumor (Stupp et al. 2005). A lack of standard of care for patients with recurrent glioblastoma further contributes to the poor prognosis for these patients.

41.1.2 Brain Metastases

In adults, brain metastases are by far the most common cause of intracranial neoplasms. Brain metastases occur in approximately 20% of the patients with systemic cancer (Achrol et al. 2019). The incidence of brain metastases has increased over the years due to therapeutic advances for patients with metastatic cancer that are associated with prolonged survival.

Brain metastases originate most commonly, in order of cumulative incidence, from lung, breast, and skin (melanoma) cancers (Tabouret et al. 2012). Although the highest numbers of brain metastases arise from the lung, melanoma has the highest propensity to metastasize to the brain (Tabouret et al. 2012).

The distribution of brain metastases correlates with blood flow and tissue volume, with 80% detected in the cerebral hemispheres, 15% in the cerebellum, and 5% in the brain stem (Delattre et al. 1988). Often, brain metastases are asymptomatic and are seen on staging brain scans. Most patients (80%) present with multiple brain metastases, and only a minority of patients (10–20%) have a solitary metastasis (Tabouret et al. 2012).

Therapeutic approaches for brain metastases are resection, radiotherapy, and systemic treatment, including immunotherapy (Hardesty and Nakaji 2016; Soffietti et al. 2017; Chen et al. 2018). Radiotherapy options can be differentiated into whole-brain radiation therapy (WBRT), which is used less frequently in recent years, and stereotactic radiotherapy (SRT), the primary choice if possible.

41.2 Imaging: Role and Dilemma

Neuroimaging is essential in the follow-up and treatment evaluation in brain tumors. Regular follow-up through neuroimaging aids clinical decision-making (Dhermain et al. 2010). Treatment is continued in patients responsive to treatment. For patient unresponsive to treatment, the treatment should be stopped. However, (beneficial) treatment reaction may appear similar to recurrent disease on conventional imaging, greatly complicating treatment decisions.

41.2.1 Role of Magnetic Resonance Imaging

41.2.1.1 Conventional MRI

Magnetic resonance imaging (MRI) is the gold standard for treatment response imaging due to its high spatial resolution, allowing detailed visualization of lesions in relation to brain anatomy. Low-grade gliomas (>90%) usually demonstrate no or limited contrast enhancement on T1-weighted imaging after gadolinium administration and are best evaluated on fluid-attenuated inversion recovery (FLAIR) and T2-weighted MRI; on the contrary, high-grade gliomas usually have contrast enhancement and are surrounded by extensive vasogenic edema (Dhermain et al. 2010). Brain metastases usually present as contrast-enhancing lesion on T1-weighted

MRI with peritumoral edema visualized on FLAIR/T2-weighted MRI. Microlesions <5 mm can already be detected with the current 1.5 and 3.0 T MRI scanners.

41.2.1.2 Advanced MRI

The rationale behind advanced MRI sequences is a better visualization of biological processes (Dhermain et al. 2010; van Dijken et al. 2017). The increased cellularity of brain tumors causes impaired diffusivity of water molecules, which is detectable by diffusion-weighted imaging. Tissue perfusion is measurable with perfusion-weighted imaging through means of detectable cerebral blood flow and volume parameters (van Dijken et al. 2019). Neovascularization, which is a hallmark of neoplasms, generally causes a measurable increase in blood flow and volume on perfusion-weighted imaging. Finally, concentrations of specific metabolites can be calculated with MR spectroscopy. Detectable metabolites include N-acetylaspartate (NAA), a marker of neuronal viability and thus intact brain tissue, choline which marks increased cellular proliferation, and lactate which demonstrates anaerobic metabolism and cell death. Increases in choline and lactate with simultaneous decrease in NAA are suggestive of tumor.

41.2.2 Role of Positron Emission Tomography

Positron emission tomography (PET) has recently been recommended by the Response Assessment in Neuro-oncology (RANO) working group to be of added value in oncological neuroimaging, thereby complementing MRI (Albert et al. 2016; Langen et al. 2017; Galldiks et al. 2019; Law et al. 2019).

41.2.2.1 FDG PET

[^{18}F]-2-fluoro-2-deoxy-D-glucose (FDG) is glucose-based and to date remains the most widely employed tracer in oncology based on an increased glucose consumption of tumors. Despite the fact that FDG is the most available tracer worldwide, its use in oncological neuroimaging is limited due to the relatively high physiological glucose metabolism of normal brain tissue (Fig. 41.1).

41.2.2.2 Amino Acid PET

Cellular proliferation associated with malignant tumors activates increased protein synthesis. Amino acids function as essential compounds of proteins, and thus amino acid transport and protein synthesis are vastly increased in malignant proliferating cells and higher compared to normal healthy tissue. Radiolabeled amino acids and amino acid analogs have different metabolic fates depending on their chemical structures (van Waarde and Elsinga 2008). Amino acid tracers are predominantly based on L-type amino acid transporters (LAT), LAT-1 and LAT-2. The most frequently used radiolabeled amino acids are [^{11}C]-methyl-L-methionine (MET) (Figs. 41.2 and 41.3), O-(2-[^{18}F]-fluoroethyl)-L-tyrosine (FET), and 3,4-dihydroxy-6-[^{18}F]-fluoro-L-phenylalanine (FDOPA) (Fig. 41.4) (Glaudemans et al. 2013; de Zwart et al. 2019).

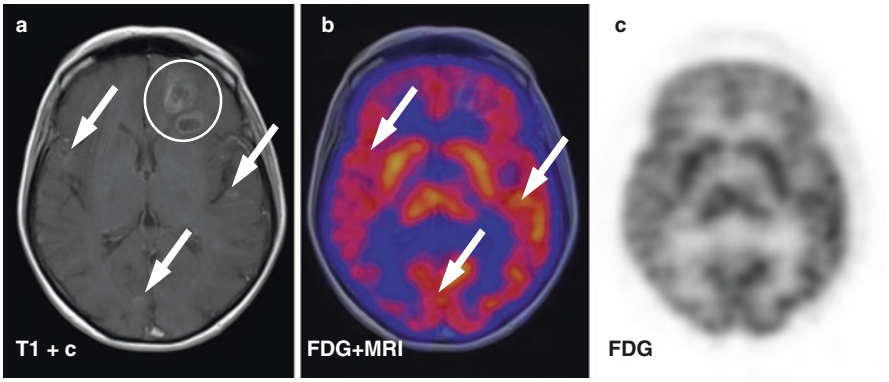

Fig. 41.1 Treatment follow-up with FDG PET in a patient with multiple brain metastases. A 62-year-old female patient with multiple brain metastases of a small cell lung cancer. Gadolinium-enhanced MRI (**a**) was performed after WBRT and demonstrated multiple contrast-enhancing lesions, with two larger lesions frontally on the left side (white circle) and several smaller lesions (white arrows). FDG PET (**b**, **c**) demonstrated high physiological uptake throughout the brain but failed to clearly localize most contrast-enhancing MRI lesions as demonstrated by the white arrows on co-registration of FDG PET images with MRI (**b**). This case demonstrates the lack of diagnostic sensitivity of FDG PET for treatment response evaluation in brain tumors

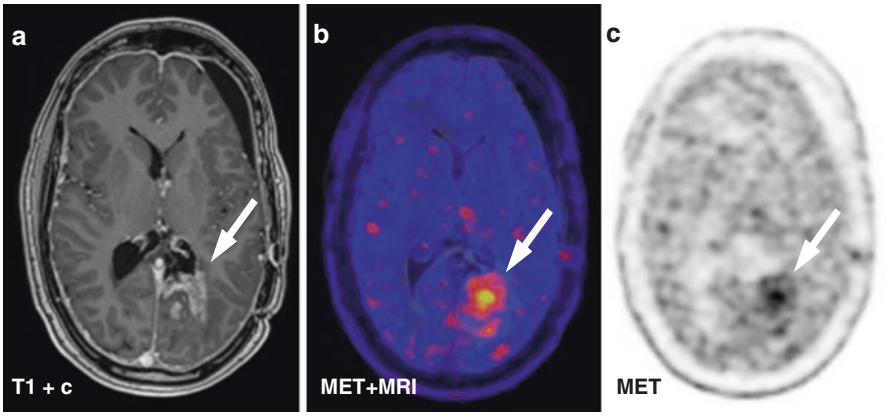

Fig. 41.2 Example of MET PET follow-up in a patient with an anaplastic astrocytoma. Case of a 49-year-old patient with an anaplastic astrocytoma (WHO grade III) after treatment with surgical resection followed by radiotherapy and temozolomide chemotherapy. One year after surgery, follow-up gadolinium-enhanced MRI (**a**) showed new contrast enhancement (white arrow). The differentiation between tumor progression and radionecrosis could not be made, and MET PET was performed (**b**, **c**). MET PET (**c**) demonstrated high tracer uptake (white arrow) suggestive of tumor progression. Co-registration of MET PET images with MRI (**b**) shows good agreement of the contrast-enhancing lesion and increased tracer uptake

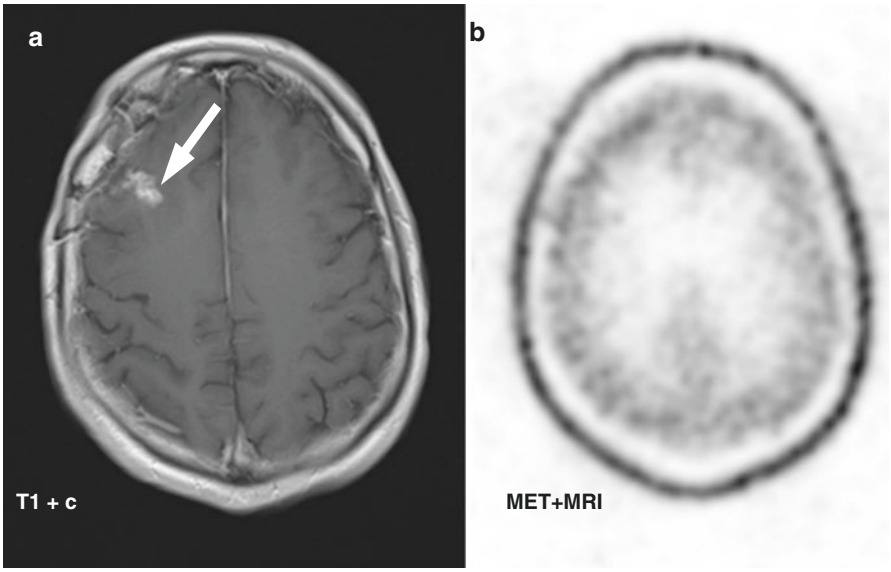

Fig. 41.3 Example of MET PET follow-up in a patient with a brain metastasis. Case of a 54-year-old male with right frontal solitary brain metastasis from a fibrosarcoma. The patient was treated with surgical resection and stereotactic radiosurgery. After treatment, follow-up gadolinium-enhanced MRI showed a new contrast-enhancing lesion (white arrow). MET PET was performed which did not demonstrate increased tracer uptake at the lesion site. The contrast enhancement was in this case shown to be due to treatment-induced changes

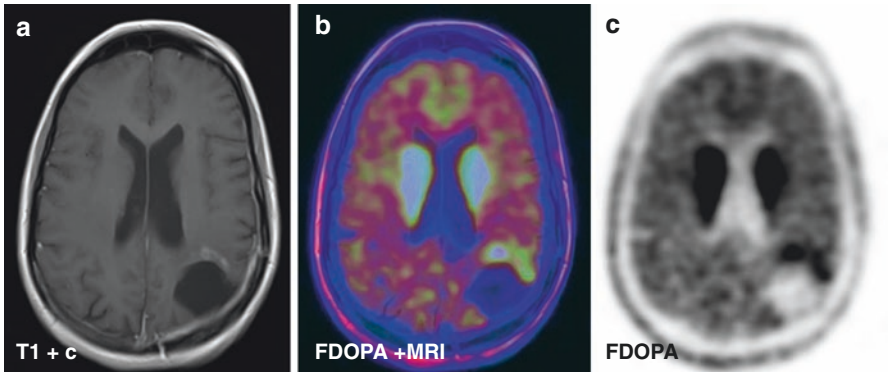

Fig. 41.4 Example of FDOPA PET follow-up in a patient with a glioblastoma. Follow-up imaging of a 26-year-old female glioblastoma patient, after surgical resection and chemoradiotherapy. Gadolinium-enhanced T1-weighted MRI (left image) 5 months after surgery was suggestive of tumor progression (white arrow). FDOPA PET was performed for other reasons (middle and right images) and demonstrated increased uptake (white arrows), also suggesting tumor progression. Co-registration of FDOPA PET and MRI (middle image) showed increased uptake at the site of enhancement on MRI. Subsequent follow-up MRI later showed further growth, confirming this case of tumor progression. The patient deceased within a year after the FDOPA PET scan

Physiological uptake of amino acid tracers in the brain is generally low, depending on anatomical region and age (Coope et al. 2007; Nagata et al. 2011). The high tumor uptake in combination with low background uptake is associated with straightforward visual assessment of amino acid PET tracers (Glaudemans et al. 2013). Therefore, the tumor detection rate and tumor delineation are thought to be better compared to FDG (Albert et al. 2016; Langen et al. 2017; Galldiks et al. 2019; de Zwart et al. 2019). Images can be interpreted visually or quantitatively. The most often used calculation method is the tumor-to-normal background ratio (T/N ratio) that compares tumor uptake to physiological uptake in the contralateral hemisphere. Uptake may also be defined by the standardized uptake value (SUV), a unit normalized to injected tracer dose per kilogram of body weight.

41.2.2.3 Other PET Tracers

In addition to amino acid PET tracers, other tracers have also been advanced. These tracers are markers of cell proliferation, such as 3′-deoxy-3′-[^{18}F]-fluorothymidine (FLT), or of the synthesis of membrane phospholipids, such as [^{11}C]-choline or [^{18}F]-fluorocholine (de Zwart et al. 2019). Both processes displayed by these tracers are active in brain tumors, thus leading to increased tracer uptake. However, these tracers are not capable of crossing an intact blood-brain barrier (BBB) (Galldiks et al. 2019). Although the BBB is usually disrupted in tumors, this is not always the case for the full extent of the tumor. To this end, only limited literature exists on these tracers. In this chapter, we will focus on amino acid PET only.

41.2.3 Dilemma of Treatment-Induced Changes

The extensive treatment regimen of malignant brain tumors, especially high-dose radiotherapy with or without concomitant chemotherapy, can produce adverse events. Damage to healthy brain tissue may lead to radiological suspicion of tumor progression (Fig. 41.3) which can even be accompanied by clinical symptoms indistinguishable from tumor progression (Brandsma et al. 2008; Thust et al. 2018). It is important to timely identify the nature of the radiological changes. True progression is indicative of failing treatment, while treatment-induced changes in fact conform with a desired response to the given treatment.

These treatment-induced changes, often called pseudoprogression in literature, are resulting from blood-brain barrier dysfunction, vasodilation, and subsequent vasogenic edema due to damage from given radiotherapy with or without chemotherapy (Brandsma et al. 2008; Thust et al. 2018). Typically, these changes occur within 3 months after treatment and will ultimately stabilize or decrease in size (Brandsma et al. 2008). Therefore, early posttreatment progression should not automatically lead to interruption of current treatment and start of second-line regimens. Delayed and longer-lasting effects, 6 months to several years after treatment, can sometimes also be seen and are then referred to as radiation necrosis.

Pseudoprogression and radiation necrosis are different clinical entities, although within the same pathological spectrum.

In high-grade gliomas, the incidence of treatment-induced changes is as high as 36% (Abbasi et al. 2018). Advances in radiotherapy planning techniques enable a high conformal dose distribution around the target volume; however, radiation dose to healthy brain tissue is unavoidable due to the infiltrative behavior of gliomas. Furthermore, treatment-induced changes are more frequent in IDH wild-type and MGMT-methylated tumors (van Dijken et al. 2019).

The incidence of treatment-induced changes in brain metastases after hypofractionated stereotactic radiotherapy (HFSRT) or stereotactic radiosurgery (SRS) is approximately 15% (Sneed et al. 2015), but some studies have suggested higher percentages (Donovan et al. 2019). Factors related to the development of radiation necrosis, especially after SRS, include dose, treated volume, and volume of the brain receiving a specific dose. An increase in the occurrence of treatment-induced changes is also expected with immunotherapy. The first studies have shown that immunotherapy alone or in addition to radiotherapy can lead to pseudoprogression and pose a new challenge for follow-up of brain metastases (Galldiks et al. 2020).

Conventional MRI cannot reliably differentiate between tumor recurrence and treatment-induced changes (van Dijken et al. 2017). Both tumor progression (Figs. 41.2 and 41.4) and treatment-induced changes (Fig. 41.3) demonstrate contrast enhancement on T1-weighted MRI with surrounding FLAIR/T2 hyperintensities. Conventional MRI, to date still the gold standard for brain tumor treatment response imaging, reached a pooled sensitivity and specificity of 68% (95% CI 51–81) and 77% (95% CI 45–93), respectively, for the detection of tumor progression in a recent meta-analysis for gliomas (van Dijken et al. 2017). Robust meta-analyses similar to those for gliomas are currently lacking for MRI in brain metastases.

To assist the clinician in the problematic differentiation of tumor progression and treatment-induced changes, the RANO criteria for gliomas and for brain metastases have been established (Wen et al. 2010; Lin et al. 2015). According to the RANO criteria, progression on conventional imaging within 3 months after chemoradiotherapy is only certain if there is new enhancement outside of the radiation field or after pathological confirmation (Wen et al. 2010). These criteria are similar for gliomas and metastases (Wen et al. 2010; Lin et al. 2015). However, in clinical practice, pathological confirmation is often not acquired in asymptomatic patients since this requires a neurosurgical intervention with a chance of morbidity. As a consequence, follow-up with imaging is usually chosen. However, this is time-consuming and can potentially expose a patient to a failing, but possibly toxic, treatment or delay the start of a second-line treatment. More advanced MRI sequences and PET tracers have therefore extensively been studied to overcome the limitations of conventional MRI (Dhermain et al. 2010; van Dijken et al. 2017, 2019; Langen et al. 2017; Galldiks et al. 2019; de Zwart et al. 2019).

41.3 Opportunities of Neuroimaging in Differentiating Tumor Progression and Treatment-Induced Changes

41.3.1 Advanced MRI

Advanced MRI sequences that have been studied for the aforementioned differentiation include diffusion-weighted imaging, detecting changes in cellular density; perfusion-weighted imaging, visualizing increased blood flow and neovascularization; and MR spectroscopy, an imaging technique capable of detecting changes in metabolites. All these advanced MRI techniques outperformed conventional MRI. Meta-analysis in high-grade gliomas showed a sensitivity and specificity for diffusion-weighted imaging of 71% (95% CI 60–80) and 86% (95% CI 76–92), respectively (van Dijken et al. 2017). For perfusion-weighted imaging, this was 87% (95% CI 82–91) and 86% (95% CI 77–91) (van Dijken et al. 2017). MR spectroscopy demonstrated the highest diagnostic accuracy with a sensitivity of 91% (95% CI 79–97) and specificity of 95% (95% CI 65–99) (van Dijken et al. 2017). As MR spectroscopy is time-consuming, with risk of movement artifacts, diffusion-weighted imaging and perfusion-weighted imaging are most often used to aid in the differentiation of tumor progression from treatment-induced changes.

Studies on the diagnostic value of advanced MRI in brain metastases after treatment are limited. Perfusion-weighted imaging and MR spectroscopy demonstrate the most promising results thus far (Chuang et al. 2016). Diagnostic accuracy seems to be in a similar good range as seen for gliomas. However, a drawback of MR spectroscopy is the relatively large voxel size, making differentiation of tumor progression from treatment-induced changes in smaller metastases difficult.

41.3.2 PET

The uptake of PET tracers is physiologically different in tumor progression and treatment-induced changes. In progressive tumors, the uptake is caused by active uptake of tracer in the tumor cells (Figs. 41.2 and 41.4). On the other hand, in treatment-induced changes, uptake is caused by passive diffusion across a disrupted BBB (Fig. 41.3). Theoretically, the uptake in tumor cells should thus exceed the uptake after radiation injury; however, there is an overlap between these uptakes. The value of PET for differentiating tumor progression from treatment-induced changes has been extensively studied in high-grade gliomas (de Zwart et al. 2019).

Recently, a meta-analysis has been conducted (de Zwart et al. 2019). This meta-analysis included 39 studies and confirmed a lower diagnostic accuracy for FDG (Fig. 41.1) than for the two most common amino acid tracers. FDG reached a sensitivity of 84% (95%CI 72–92) and specificity of 84% (95%CI 69–93), while FET, with a sensitivity of 90% (95%CI 81–95) and a specificity of 85% (95%CI 71–93), and MET (Figs. 41.2 and 41.3), with a sensitivity and specificity of 93% (95%CI 80-98) and 82% (95%CI 68-91), respectively, performed significantly better (de Zwart et al. 2019). FDOPA is a less studied tracer (Fig. 41.4), with only four known

studies being published, but demonstrates comparable diagnostic accuracy with a sensitivity ranging from 85% to 100% and specificity ranging from 72% to 100% (Lapa et al. 2014; Karunanithi et al. 2013; Paquet et al. 2017; Herrmann et al. 2014).

The usefulness of FDG PET is very limited in brain metastases (Fig. 41.1). Studies have shown that FDG PET only marginally improves accurate differentiation between tumor progression and treatment-induced changes after ambiguous MRI (Chao et al. 2001; Belohlávek et al. 2003). As expected, the accuracy of amino acid PET is superior to FDG PET.

Several studies have confirmed that a difference in FET T/N ratios can quantitatively distinguish metastatic progression from treatment-induced changes (Galldiks et al. 2012; Romagna et al. 2016; Ceccon et al. 2017). However, the number of patients studied with FET PET ($N = 126$) is much smaller than for MET PET.

For MET PET, most studies had a relatively high sensitivity, specificity, and diagnostic accuracy (>85%) in common, with advantages over conventional imaging (Figs. 41.2 and 41.3) (Terakawa et al. 2008; Yomo and Oguchi 2017; Okamoto et al. 2010; Yamane et al. 2010; Tsuyuguchi et al. 2003). However, a considerable overlap in the uptake values of methionine in progressing tumor and treatment-induced change occurs (Minamimoto et al. 2015).

A visual analysis of 83 lesions in 32 patients also demonstrated positive results for FDOPA (Lizarraga et al. 2014). In another study, among 13 patients of whom 3 had histologically confirmed treatment-induced changes, there was a visual difference in FDOPA uptake between recurrent or progressive metastases and treatment-induced changes (Papin-Michault et al. 2016). This study additionally demonstrated a difference in LAT-1 expression between tumor progression cases and treatment-induced changes, explaining the difference in FDOPA uptake (Papin-Michault et al. 2016). Interestingly, FDOPA outperformed perfusion-weighted imaging in a study among 42 patients with brain metastases after SRS (Cicone et al. 2015).

41.4 Limitations and Future Perspectives of MRI and PET

MRI and PET seem to perform similar in the differentiation of treatment-induced changes from tumor progression. However, only few studies have compared MRI and PET directly.

A study by Kim et al. (2010) stated that perfusion-weighted MRI is superior in distinguishing a recurrence of high-grade glioma from radiation necrosis compared to MET. Dandois et al. (2010) also found that perfusion-weighted MRI had an at least similar diagnostic accuracy to MET in differentiating tumor recurrence and treatment-induced changes. However, FDOPA was suggested to outperform perfusion-weighted MRI (Cicone et al. 2015), and another study also demonstrated that amino acid PET is possibly superior over perfusion-weighted MRI (Tomura et al. 2017).

The diagnostic accuracy of the different amino acid PET tracers seems comparable, although FDOPA is somewhat understudied compared to MET and FET PET. Most experience is gathered with MET. However, MET is impractical since it

demands a cyclotron due to its very short half-life (20 min). Fluorine-18-labeled FET has gained ground due to its longer half-life (109.7 min).

There is an urgent need for uniform scanning protocols and quantification methods for both advanced MRI and amino acid PET. Furthermore, few data are available on interobserver agreement in the interpretation of these advanced MRI sequences and PET studies. Amino acid PET can usually relatively easily be interpreted visually, but there is a lack of consensus on the used reference region for calculation of T/N ratios. Local variations in tracer uptake between different reference regions may significantly alter results. With T/N ratios still being the most reported quantitative parameter, this is troublesome. Future studies should thus focus on establishing robust guidelines for analysis and quantification methods for amino acid PET in brain tumors.

It has been suggested that the recent development of hybrid PET/MRI cameras could lead to a jump forward in the imaging of brain tumors. Combining both modalities might overcome a number of individual limitations and avoids the necessity of additional scanning. This would enable an absolute match between tissue information of both modalities under the same physiological conditions and may thus lead to better localization of the PET signal within the soft tissues. However, the economic cost of hybrid PET/MRI scanners is substantial. The first studies have been published and indeed demonstrate the feasibility of using combined PET/MRI machines (Hojjati et al. 2018; Deuschl et al. 2018). However, these studies are limited to FDG PET (Hojjati et al. 2018), which has insufficient value in brain tumor imaging, and carbon-bound MET PET (Deuschl et al. 2018), which is not feasible in many centers. Therefore, more PET/MRI studies with emphasis on treatment evaluation of gliomas and brain metastases using fluorine-bound amino tracers are desired.

41.5 Summary

Treatment-induced changes are a common phenomenon among both treated gliomas and brain metastases. Conventional MRI is not able to differentiate tumor progression and treatment-induced changes. Both advanced MRI techniques and amino acid PET provide additional information that can aid the clinician in decision-making following treatment. Combining all evidence that we presented in this chapter, there does not seem to be a preferred advanced MRI or PET imaging method to differentiate tumor progression from treatment-induced changes.

References

Abbasi AW, Westerlaan HE, Holtman GA, Aden KM, van Laar PJ, van der Hoorn A (2018) Incidence of tumour progression and pseudoprogression in high-grade gliomas: a systematic review and meta- analysis. Clin Neuroradiol 28:401–411

Achrol A, Rennert R, Anders C et al (2019) Brain metastases. Nat Rev Dis Primers 5(1):5

Albert NL, Weller M, Suchorska B et al (2016) Response assessment in neuro-oncology working group and european association for neuro-oncology recommendations for the clinical use of PET imaging in gliomas. Neuro-Oncology 18:1199–1208

Bell EH, Zhang P, Fisher BJ et al (2018) Association of MGMT promoter methylation status with survival outcomes in patients with high-risk glioma treated with radiotherapy and temozolomide: an analysis from the NRG oncology/RTOG 0424 trial. JAMA Oncol 4(10):1405–1409

Belohlávek O, Simonová G, Kantorová I, Novotný J Jr, Liscák R (2003) Brain metastases after stereotactic radiosurgery using the leksell gamma knife: can FDG PET help to differentiate radionecrosis from tumour progression? Eur J Nucl Med Mol Imaging 30(1):96–100

Binabaj MM, Bahrami A, ShahidSales S et al (2018) The prognostic value of MGMT promoter methylation in glioblastoma: a meta-analysis of clinical trials. J Cell Physiol 233(1):378–386

Boonzaier NR, Larkin TJ, Matys T et al (2017) Multiparametric MR imaging of diffusion and perfusion in contrast-enhancing and nonenhancing components in patients with glioblastoma. Radiology 284(1):180–190

Brandsma D, Stalpers L, Taal W, Sminia P, van den Bent MJ (2008) Clinical features, mechanisms, and management of pseudoprogression in malignant gliomas. Lancet Oncol 9:453–461

Ceccon G, Lohmann P, Stoffels G et al (2017) Dynamic O-(2-18F-fluoroethyl)-L-tyrosine positron emission tomography differentiates brain metastasis recurrence from radiation injury after radiotherapy. Neuro-Oncology 19(2):281–288

Chao ST, Suh JH, Raja S, Lee SY, Barnett G (2001) The sensitivity and specificity of FDG PET in distinguishing recurrent brain tumor from radionecrosis in patients treated with stereotactic radiosurgery. Int J Cancer 96(3):191–197

Chen L, Douglass J, Kleinberg L et al (2018) Concurrent immune checkpoint inhibitors and stereotactic radiosurgery for brain metastases in non-small cell lung cancer, melanoma, and renal cell carcinoma. Int J Radiat Oncol Biol Phys 100(4):916–925

Chuang MT, Liu YS, Tsai YS, Chen YC, Wang CK (2016) Differentiating radiation-induced necrosis from recurrent brain tumor using MR perfusion and spectroscopy: a meta-analysis. PLoS One 11(1):e0141438

Cicone F, Minniti G, Romano A et al (2015) Accuracy of F-DOPA PET and perfusion-MRI for differentiating radionecrotic from progressive brain metastases after radiosurgery. Eur J Nucl Med Mol Imaging 42(1):103–111

Coope DJ, Cizek J, Eggers C et al (2007) Evaluation of primary brain tumors using 11C-methionine PET with reference to a normal methionine uptake map. J Nucl Med 48(12):1971–1980

Dandois V, Rommel D, Renard L, Jamart J, Cosnard G (2010) Substitution of 11C-methionine PET by perfusion MRI during the follow-up of treated high-grade gliomas: preliminary results in clinical practice. Neuroradiology 37:89–97

de Zwart PL, van Dijken BRJ, Holtman GA et al (2019) Diagnostic accuracy of positron emission tomography tracers for the differentiation of tumor progression from treatment-related changes in high-grade glioma: a systematic review and meta-analysis. J Nucl Med 119:233809

DeAngelis LM (2001) Brain tumors. N Engl J Med 344:114–123

Delattre JY, Krol G, Thaler HT, Posner JB (1988) Distribution of brain metastases. Arch Neurol 45(7):741–744

Deuschl C, Kirchner J, Poeppel TD et al (2018) 11C-MET PET/MRI for detection of recurrent glioma. Eur J Nucl Med Mol Imaging 45(4):593–601

Dhermain FG, Hau P, Lanfermann H, Jacobs AH, van den Bent MJ (2010) Advanced MRI and PET imaging for assessment of treatment response in patients with gliomas. Lancet Neurol 9:906–920

Donovan EK, Parpia S, Greenspoon JN (2019) Incidence of radionecrosis in single-fraction radiosurgery compared with fractionated radiotherapy in the treatment of brain metastasis. Curr Oncol 26(3):e328–e333

Galldiks N, Stoffels G, Fills CP et al (2012) Role of O-(2-(18)F-fluoroethyl)-L-tyrosine PET for differentiation of local recurrent brain metastasis from radiation necrosis. J Nucl Med 53(9):1367–1374

Galldiks N, Lohmann P, Albert NL et al (2019) Current status of PET imaging in neuro-oncology. Neuro-Oncol Adv 1(1):vdz010

Galldiks N, Kocher M, Ceccon G et al (2020) Imaging challenges of immunotherapy and targeted therapy in patients with brain metastases: response, progression, and pseudoprogression. Neuro-Oncology 22(1):17–30

Glaudemans AWJM, Enting RH, Heesters MAAM et al (2013) Value of 11C-methionine PET in imaging brain tumours and metastases. Eur J Nucl Med Mol Imaging 40:615–635
Hardesty D, Nakaji P (2016) The current and future treatment of brain metastases. Front Surg 3(30):1–7
Herrmann K, Czernin J, Cloughesy T et al (2014) Comparison of visual and semiquantitative analysis of 18F-FDOPA- PET/CT for recurrence detection in glioblastoma patients. Neuro-Oncology 16:603–609
Hojjati M, Badve C, Garg V et al (2018) Role of FDG-PET/MRI, FDG-PET/CT, and dynamic susceptibility contrast perfusion mri in differentiating radiation necrosis from tumor recurrence in glioblastomas. J Neuroimaging 28:118–125
Karunanithi S, Sharma P, Kumar A et al (2013) Comparative diagnostic accuracy of contrast-enhanced MRI and 18F-FDOPA PET-CT in recurrent glioma. Eur Radiol 23:2628–2635
Kim YH, Oh SW, Lim YJ et al (2010) Differentiating radiation necrosis from tumor recurrence in high-grade gliomas: assessing the efficacy of 18F-FDG PET, 11C-methionine PET and perfusion MRI. Clin Neurol Neurosurg 112(9):758–765
Langen KJ, Galldiks N, Hattingen E, Shah NJ (2017) Advances in neuro-oncology imaging. Nat Rev Neurol 13:279–289
Lapa C, Linsenmann T, Monoranu CM et al (2014) Comparison of the amino acid tracers 18F-FET and 18F-DOPA in high-grade glioma patients. J Nucl Med 55:1611–1616
Law I, Albert NL, Arbizu J et al (2019) Joint EANM/EANO/RANO practice guidelines/SNMMI procedure standards for imaging of gliomas using PET with radiolabelled amino acids and [18F]FDG: version 1.0. Eur J Nucl Med Mol Imaging 46:540–557
Lin NU, Lee EQ, Aoyama H et al (2015) Response assessment criteria for brain metastases: proposal from the RANO group. Lancet Oncol 16(6):e270–e278. https://doi.org/10.1016/S1470-2045(15)70057-4
Lizarraga KJ, Allen-Auerbach M, Czernin J et al (2014) (18)F-FDOPA PET for differentiating recurrent or progressive brain metastatic tumors from late or delayed radiation injury after radiation treatment. J Nucl Med 55(1):30–36
Louis DN, Perry A, Reifenberger G et al (2016) The 2016 World Health Organization classification of tumors of the central nervous system: a summary. Acta Neuropathol 131:803–820
Minamimoto R, Saginoya T, Kondo C, Tomura N, Ito K, Matsuo Y et al (2015) Differentiation of brain tumor recurrence from post-radiotherapy necrosis with 11C-methionine PET: visual assessment versus quantitative assessment. PLoS One 10(7):e0132515
Miranda-Filho A, Pineros M, Soerjomataram I et al (2017) Cancers of the brain and CNS: global patterns and trends in incidence. Neuro-Oncology 19(2):270–280
Nagata T, Tsuyuguchi N, Uda T et al (2011) Examination of 11C-methionine metabolism by the standardized uptake value in the normal brain of children. J Nucl Med 52:201–205
Okamoto S, Shiga T, Hattori N, Kubo N, Takei T, Katoh N et al (2010) Semiquantitative analysis of C-11 methionine PET may distinguish brain tumor recurrence from radiation necrosis even in small lesions. Ann Nucl Med 25(3):213–220
Ostrom QT, Cioffi G, Gittleman H et al (2019) BTRUS statistical report: primary brain and other central nervous system tumors diagnosed in the United States in 2012–2016. Neuro Oncol 21(Suppl 5):v1–v100
Papin-Michault C, Bonnetaud C, Dufour M et al (2016) Study of LAT1 expression in brain metastases: towards a better understanding of the results of positron emission tomography using amino acid tracers. PLoS One 11(6):e0157139
Paquet M, Doyen J, Mondot L et al (2017) Value of early and delayed imaging for 18F-FDOPA PET high grade gliomas evaluation [abstract]. Eur J Nucl Med Mol Imaging 44:S642–S643
Rogers TW, Toor G, Drummond K et al (2018) The 2016 revision of the WHO classification of central nervous system tumours: retrospective application to a cohort of diffuse gliomas. J Neuro-Oncol 137(1):181–189
Romagna A, Unterrainer M, Schmid-Tannwald C et al (2016) Suspected recurrence of brain metastases after focused high dose radiotherapy: can [18F]FET- PET overcome diagnostic uncertainties? Radiat Oncol 11(1):139

Sanai N, Berger MS (2008) Glioma extent of resection and its impact on patient outcome. Neurosurgery 62(4):753–764

Sneed P, Mendez J, Vemer-van den Hoek J et al (2015) Adverse radiation effect after stereotactic radiosurgery for brain metastases: incidence, time course, and risk factors. J Neurosurg 123(2):373–386

Soffietti R, Abacioglu U, Baumert B et al (2017) Diagnosis and treatment of brain metastases from solid tumors: guidelines from the European Association of Neuro-Oncology (EANO). Neuro-Oncology 19(2):162–174

Stupp R, Mason WP, van den Bent MJ et al (2005) Radiotherapy plus concomitant and adjuvant temozolomide for glioblastoma. N Engl J Med 352:987–996

Tabouret E et al (2012) Recent trends in epidemiology of brain metastases: an overview. Anticancer Res 32:4655–4662

Terakawa Y, Tsuyuguchi N, Iwai Y, Yamanaka K, Higashiyama S, Takami T et al (2008) Diagnostic accuracy of 11C-methionine PET for differentiation of recurrent brain tumors from radiation necrosis after radiotherapy. J Nucl Med 49(5):694–699

Thust SC, Van Den Bent MJ, Smits M (2018) Pseudoprogression of brain tumors. J Magn Reson Imaging 48:571–589

Tomura N, Kokubun M, Saginoya T et al (2017) Differentiation between treatment-induced necrosis and recurrent tumors in patients with metastatic brain tumors: comparison among 11C-methionine-PET, FDG-PET, MR permeability imaging, and MRI-ADC—preliminary results. AJNR 38(8):1520–1527

Tsuyuguchi N, Sunada I, Iwai Y et al (2003) Methionine positron emission tomography of recurrent metastatic brain tumor and radiation necrosis after stereotactic radiosurgery: is a differential diagnosis possible? J Neurosurg 98(5):1056–1064

van den Bent MJ, Baumert B, Erridge SC et al (2017) Interim results from the CATNON trial (EORTC study 26053-22054) of treatment with concurrent and adjuvant temozolomide for 1p/19q non-co-deleted anaplastic glioma: a phase 3, randomised, open-label intergroup study. Lancet 390(10103):1645–1653

van Dijken BRJ, van Laar PJ, Holtman GA, van der Hoorn A (2017) Diagnostic accuracy of magnetic resonance imaging techniques for treatment response evaluation in patients with high-grade glioma, a systematic review and meta-analysis. Eur Radiol 27:4129–4144

van Dijken BRJ, van Laar PJ, Smits M et al (2019) Perfusion MRI in treatment evaluation of glioblastomas: clinical relevance of current and future techniques. J Magn Reson Imaging 49:11–22

van Waarde A, Elsinga PH (2008) Proliferation markers for the differential diagnosis of tumor and inflammation. Curr Pharm Des 14(31):3326–3339

Weller M, van den Bent MJ, Tonn JC et al (2017) European Association for Neuro-Oncology (EANO) guideline on the diagnosis and treatment of adult astrocytic and oligodendroglial gliomas. Lancet Oncol 18(6):e315–e329

Wen PY, Macdonald DR, Reardon DA et al (2010) Updated response assessment criteria for high-grade gliomas: response assessment in neuro-oncology working group. J Clin Oncol 28:1963–1972

Yamane T, Sakamoto S, Senda M (2010) Clinical impact of 11C-methionine PET on expected management of patients with brain neoplasm. Eur J Nucl Med Mol Imaging 37(4):685–690

Yan JL, van der Hoorn A, Larkin TTJ et al (2017) Extent of resection of peritumoral diffusion tensor imaging-detected abnormality as a predictor of survival in adult glioblastoma patients. J Neurosurg 126(1):234–241

Yan JL, Li C, Boonzaier NR et al (2019) Multimodal MRI characteristics of the glioblastoma infiltration beyond contrast enhancement. Ther Adv Neurol Disord 12:1756286419844664

Yomo S, Oguchi K (2017) Prospective study of 11C-methionine PET for distinguishing between recurrent brain metastases and radiation necrosis: limitations of diagnostic accuracy and long-term results of salvage treatment. BMC Cancer 17(1):713